LASER INTERFEROMETER GRAVITATIONAL WAVE OBSERVATORY

Temporal

LIGO Laboratory / LIGO Scientific Collaboration

LIGO-T1600463-v1 *LIGO* October 19, 2016

Guestimation of large angle scattering

Hiro Yamamoto

Distribution of this document:
LIGO Scientific Collaboration

This is an internal working note
of the LIGO Project.

California Institute of Technology
LIGO Project – MS 100-36
1200 E. California Blvd.
Pasadena, CA 91125
Phone (626) 395-2129
Fax (626) 304-9834
E-mail: info@ligo.caltech.edu

Massachusetts Institute of Technology
LIGO Project – NW22-295
185 Albany St
Cambridge, MA 02139
Phone (617) 253-4824
Fax (617) 253-7014
E-mail: info@ligo.mit.edu

LIGO Hanford Observatory
P.O. Box 1970
Mail Stop S9-02
Richland WA 99352
Phone 509-372-8106
Fax 509-372-8137

LIGO Livingston Observatory
P.O. Box 940
Livingston, LA 70754
Phone 225-686-3100
Fax 225-686-7189

http://www.ligo.caltech.edu/

1 Introduction

There are not enough data nor knowledge to calculate the large angle scattering off by mirrors in LIGO interferometers. This makes it difficult to understand the cause of the loss in the arm and to predict various noises induced by stray lights. This document summarizes information which will be helpful to guestimate the large angle scattering, and to understand what are missing for more accurate guestimation.

In order to estimate the arm loss, the entire angular region by a mirror scattering need to be measured and understood. In-situ measurement is very difficult because very small solid angles are covered at only handful of locations and the extrapolation to estimate the rest of the large solid angle is very ambiguous.

The large angle scattering information of mirrors measured before the installation is also limited. The assumption of a constant BRDF or Lambertian scattering does not apply for the reflection by the test mass with superpolish and smooth coating.

The BRDF measurement is usually limited to down to several degrees from the incident angle. The scattering toward very close to the incident angle is estimated by assuming smooth interpolation, but the angular distribution in this region depends on the smoothness of the surface and on the size and number of discrete defects.

One direct measurement down to the direction very close to the incident beam is done by using an integrating sphere. In the last, the measurement was done covering between 1° to 75° from the incident direction. The data shows strong correlation between the polished surface RMS and the measured TIS. A few % of the surface points scanned by a small laser (300 μm) show large scattering, and these discrete defects increase the average loss by 30%. It was assumed that the scattering into the uncovered region less than 1° is negligible. But, large defects tend to scatter more close to the incident direction and the integrating sphere data could be still underestimating the total loss from a mirror.

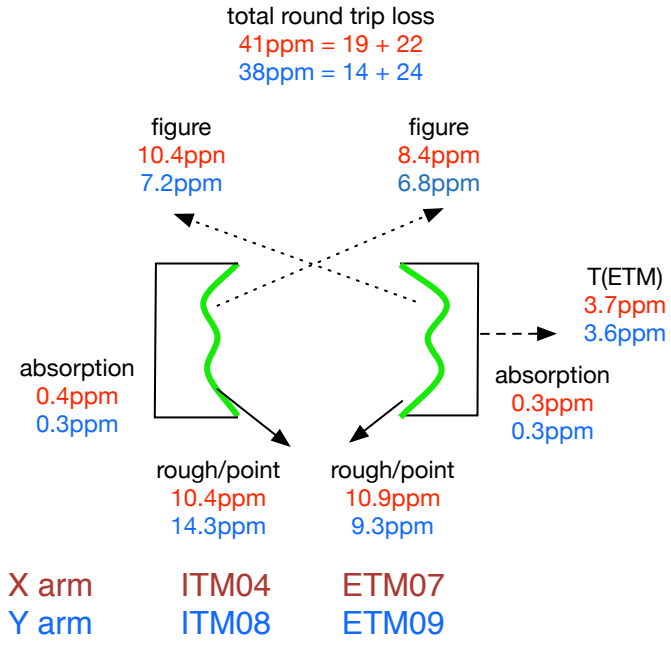

L1 loss budget

2 Basic

2.1 Geometry of the arm

The basic geometry of the LIGO arm is shown below. Those parts of the field scattered by one test mass and arriving outside of the other test mass are the loss. The opening angle of ETM seen from ITM is 43μrad and the solid angle, π radius^2, is only $(0.17/4000)^2 = 2\text{x}10^{-9}$ of the full solid angle 2 π. Scattering by aberrations are generally wide spread and almost all scattered fields are lost.

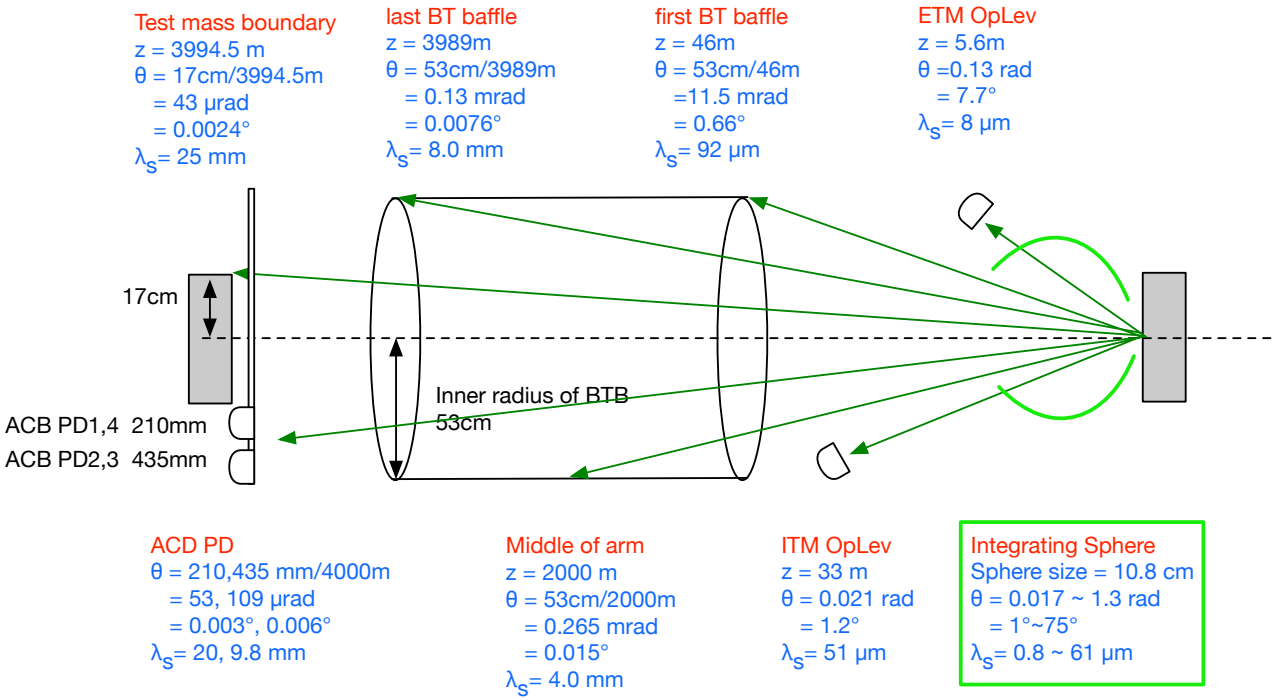

2.2 Scattering by mirror surface aberration

2.2.1 Basic

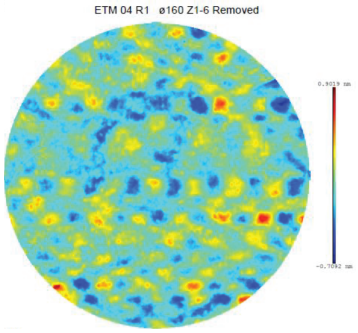

(1) Surface after polishing by ASML
Aperture size 160mm
RMS = 0.1732nm, PV=1.611nm

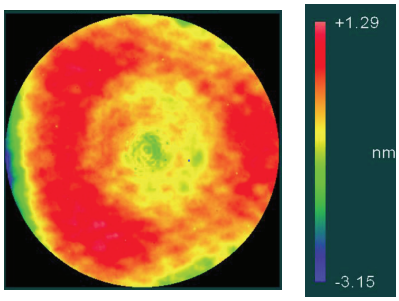

(2) Surface after multilayer coating by ison spattering
Aperture160mm
RMS = 0.563nm, PV=4.436nm

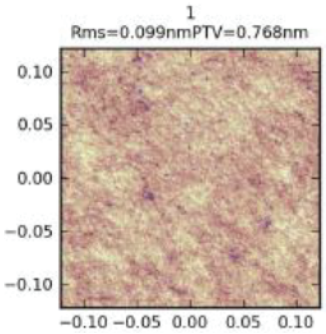

(3) Surface after polishing measured by PMM(phase measuring microscope) with magnification of 50.
0.25mm x 0.25mm square near center.
RMS = 0.099nm, PV=0.768nm

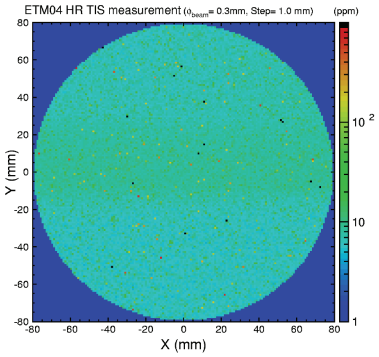

(4) Reflectance measured by an integrating sphere with the scattering angle larger than 1°. The size of the laser is 0.3mm, with spacing 1mm.
RMS using all data points is 98ppm. RMS is 20ppm after excluding 15 points with reflectance > 1000ppm.

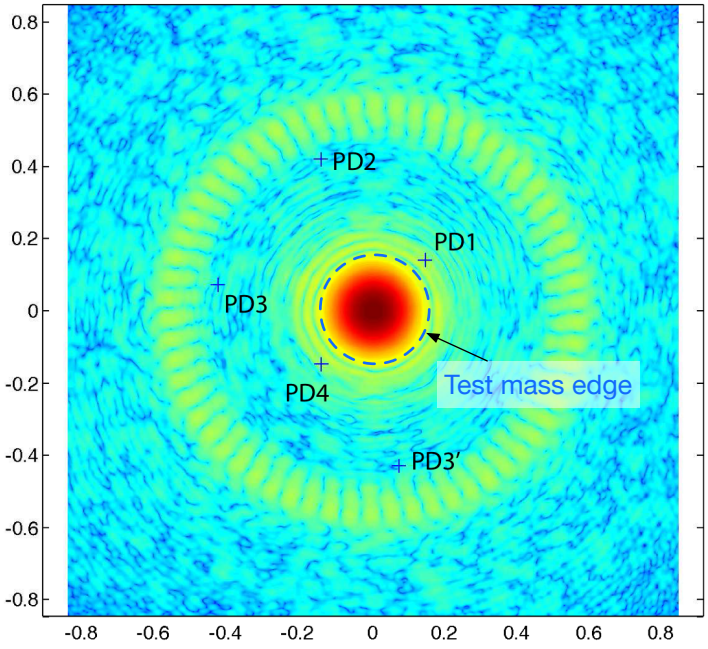

When a field is reflected by a finite size mirror with aberration – deviation from an idealistic perfect spherical surface, there are four kinds of disturbance induced in the reflected field, as is discussed in Sec. 2.2.2~2.2.5.

When considering only the surface height deformation, the aberration can be characterized by a real number function, h(x,y), which gives the surface height at each location, (x,y), on the mirror surface coated area. This function can be expressed by a combination of 1)sum of Zernike polynomials, 2)smooth structure which can be characterized by power spectral density, and 3)discrete random distortions.

1) The sum of Zernike polynomials represents structures with long spatial wavelength, like curvature mismatch, astigmatism or spherical aberration.
2) The smooth structure characterized by PSD corresponds to small size height variation of the polished and coated surfaces with short spatial wavelength. This kind of aberration is universal all over one mirror surface, i.e., similar PSD at different locations on one mirror. The reflected fields by this kind of structure – variation with same spatial frequency at different location – interferer each other to make the far field pointing to large angle.
3) The discrete random distortion corresponds to defects populated on one mirror surface without any regularity, i.e., reflected fields by separate defects do not interferer, and the far fields are just sum of spherical waves without specific interference pattern.

The phasemap measured by a Fizeau interferometer usually gives the height with spatial resolution of fraction of mm. It is difficult to measure structures with shorter spatial wavelength, and other methods like PMM (Phase Measuring Microscope). Zygo used PMM to measure the aLIGO test mass polished surface down to 1μm.

For other cases, including variation of reflectance and anomalies inside of coating layers, same formulations can be used by using a complex function, instead of real function. E.g., the effect of a small area with a different absorption can be calculated using an imaginary value for h(x,y).

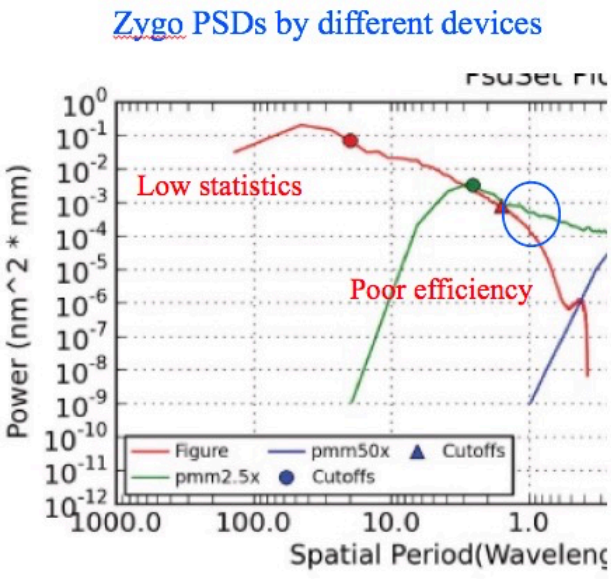

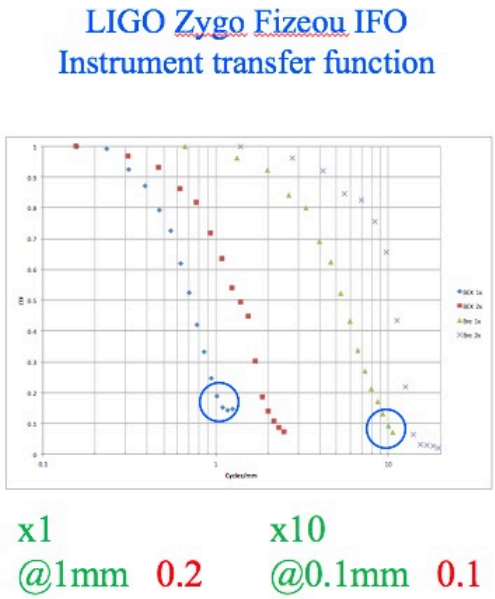

2.2.2 Diffraction by finite mirror aperture

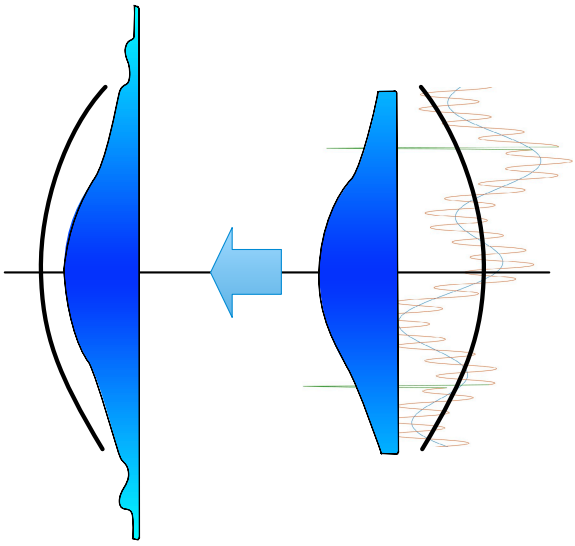

See Sec. "Diffraction, Finite size mirror effect, Airy Ring"

Due to the diffraction induced by the size of the test masses, the round trip loss of a aLIGO cavity is 1.9ppm for the mirror coated area aperture 32.6cm. These are twice as large compared to the loss, $\exp(-2\ \text{radius}^2 / w(\text{ITM})^2) + \exp(-2\ \text{radius}^2 / w(\text{ETM})^2)$, assuming a pure Gaussian shape with beam size w on both test masses.

The angular distribution (θ=r/L) of the energy flow or BRDF is cos(k aperture θ) / θ^3, to be compared with the Gaussian case $\exp(-2(L/w)^2\ \theta^2)$. Although the total energy loss due to the diffraction is small, O(1ppm), the diffraction tail is important in the forward direction around the test mass boundary, like ACD PD.

2.2.3 Long spatial wave length surface figure error

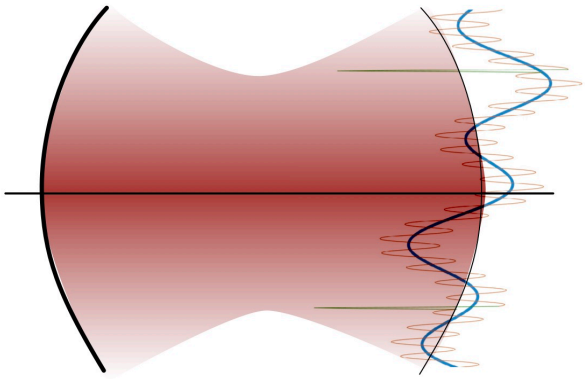

See Sec.3.4 "Scattering power distribution by continuous aberrations", Sec. 3.5 "Spatial wavelength of aberration and cavity loss" and Sec. 4.2 "FFT field calculation with phasemap and PSD and BRDF".

Surface figure errors with long spatial wavelength, like curvature mismatch, astigmatism or spherical aberration, scattered field back into the cavity, and the main effect is the distortion of the resonating mode in the cavity.

This aberration also amplifies the tail of the field, by the excitation of higher order modes with longer tails or by the coherent scattering to larger angle, a.la. Sec.2.2.3.

The aLIGO arm losses with installed mirror phasemaps are calculated to be around 15~20ppm, to be compared with 1.9ppm for the arm without phasemap.

For the fields outside of the test mass, this scattering plays important role in $r < 0.8$m or $\theta < 0.01°$ or $\lambda_s > 5$mm. The field in the cavity is calculated by numerical simulations with measured phasemaps. When there are any structures in the phasemaps, simulations need to set the resolution better than that. E.g., the spiral pattern on the ETMs has a spacing of 8mm, which shows peak at radius of 50-60cm, and the simulation needs to have resolution of 1-2mm to calculate this effect properly.

2.2.4 Short wavelength surface-wde aberration

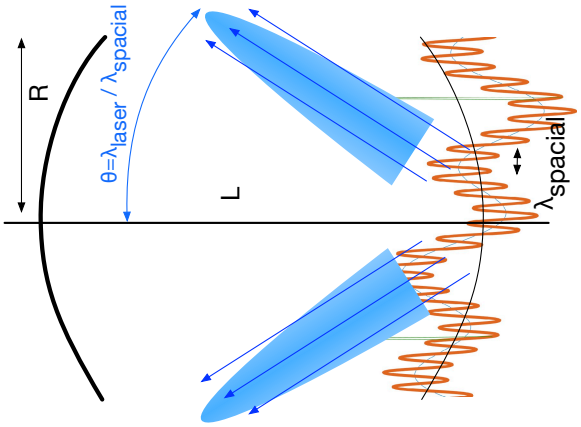

See Sec. 3.4 "Scattering power distribution by continuous aberrations", Sec. 3.5 "Spatial wavelength of aberration and cavity loss".

When a certain periodic structure exists over a region larger than its spatial wavelength, λs, fields reflected by the structure interferers after long distance propagation. The structure with spatial wavelength of λs scatters field toward an angle of $\theta = \lambda_{laser} / \lambda_{spatial}$. When L θ is larger than the mirror radius R, then it is lost.

The scattered beam has broadening and the scattering region is not at fixed narrow area, so there is no clear cutoff spatial wavelength to quantify the loss. The aberration with λs < 2mm are almost surely lost, and the loss estimation by the golden rule works. So the combination of numerical simulation with phasemaps with resolution of O(1mm) and the estimation by measured RMS (λs < 2mm) + golden rule or any direct measurement of TIS for the corresponding region is the way to calculate the total loss, except the point scattering.

2.2.5 Small size random aberrations

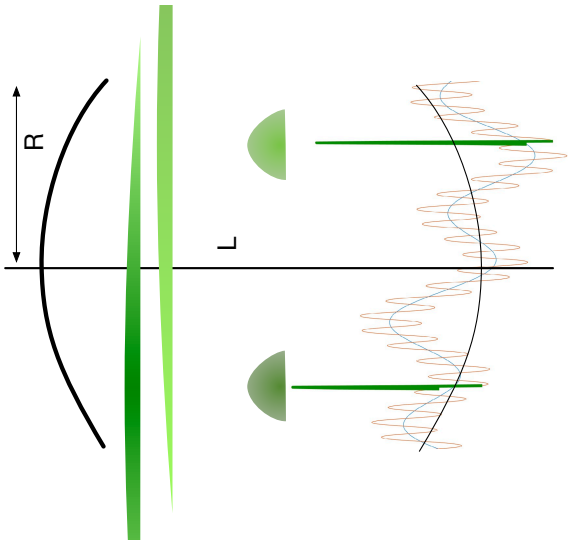

See Sec. 3.6 "Scattering power distribution by isolated aberrations or point defects" and Sec. 3.2 "Total scattered power and RMS and the GOLDEN RULE"

Fields scattered by randomly located point defects do not interfere at far distance, so the distribution of the total disturbance after long propagation is essentially a superposition of spherical waves with uncorrelated relative phases.

The total energy scattered by one small defect is proportional to the power of the incident field interacting with the defect size. When a Gaussian field interacts with a circular defect with radius of d, the scattered energy is proportional to $(d/w)^2$, which is very small $(1\mu m/5cm)^2 = O(10^{-9})$. In order to scatter several 10ppm by random defects, the total area should be $(0.15mm)^2$.

The angular distribution of the reflected field depends on the size of the defect. If small defects clusters together, the angular distribution from these clustered defects look like the reflection by one defect. This difference of the angular distribution by the shape of the reflecting defect introduce uncertainties of factor of several to estimate the total scattering by using the power at the large angle.

The solid angle of the mirror with radius R located distance L from the scattering source is $2\pi R^2 / L^2$, and is a very small faction, $(0.17 \text{ m} / 4\text{km})^2 = O(10^{-9})$, of the half hemisphere solid angle 2π. So the target mirror size can be neglected when calculating the loss by random point defects.

The disturbance of the field in the cavity by point defects is so small that it can be neglected. Tiny ripples in the cavity field induced by a point defect is axisymmetric around the cavity axis, with rings with spacing determined by the distance of the defect relative to the mirror center.

2.3 Smooth roughness and random defects

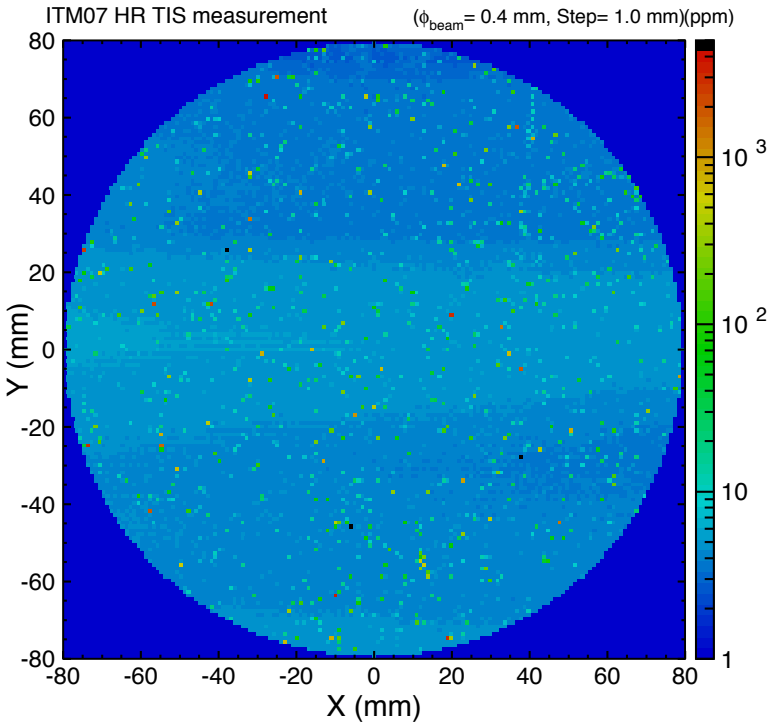

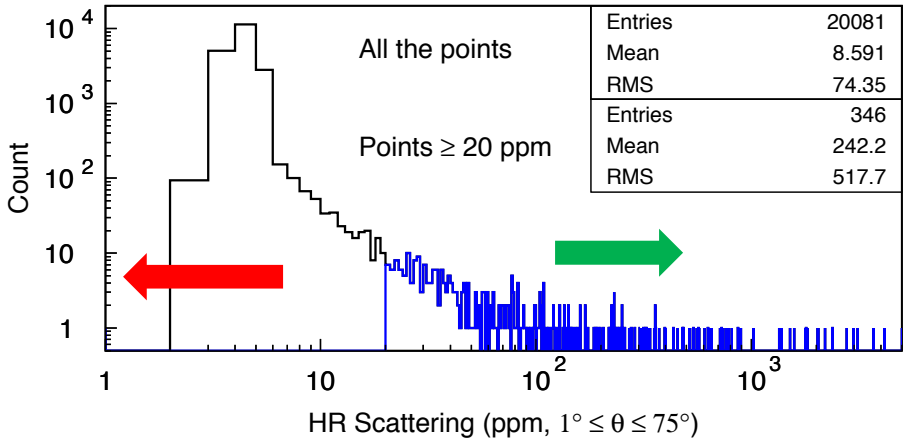

Continuous roughness

Point scattering

$$\frac{dP}{P_{in}} = \left(\frac{4\pi\sigma(w_0)}{\lambda}\right)^2 + < n > dS \left(\frac{4\pi\Delta}{\lambda}\right)^2$$

- σ(w) : rms with f > 1/w
- <n> : density of point defects
- dS : size of point defect
- Δ : characteristics of point defect

G1601678-4

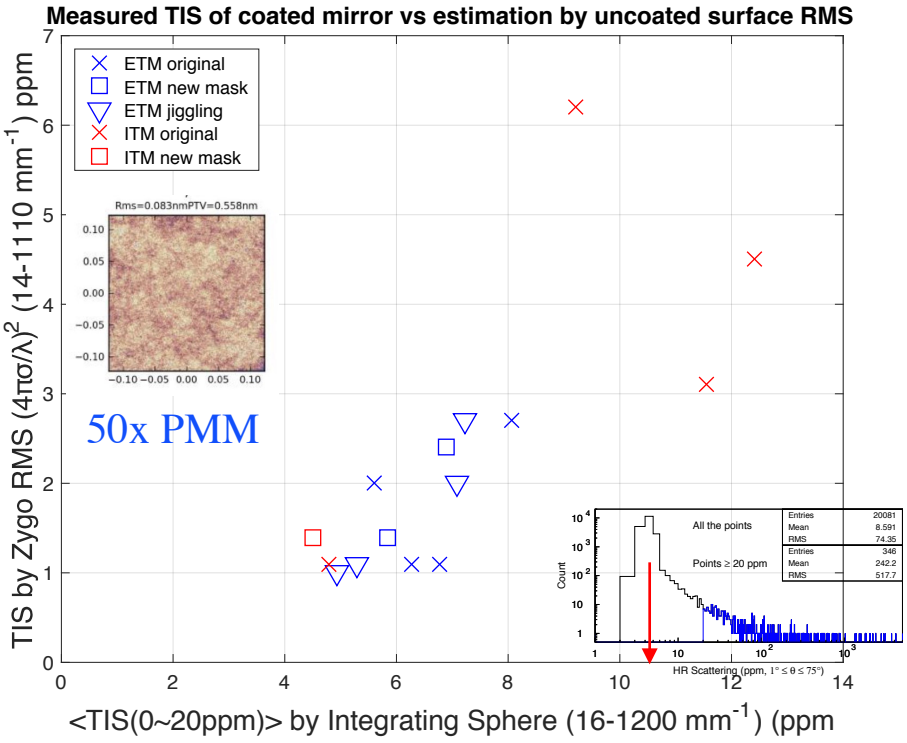

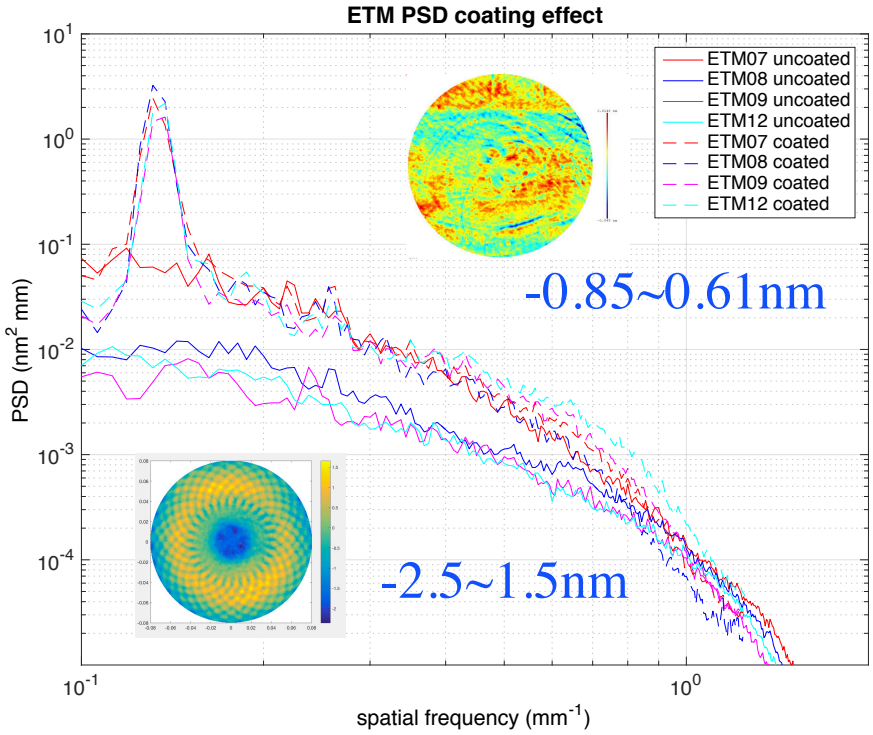

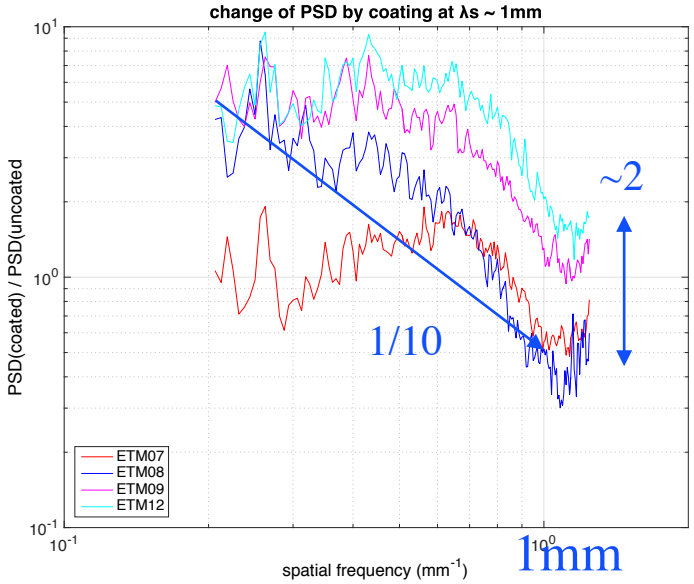

2.4 BRDF, PSD, Lambertian, data coverage, etc

See Sec. 4.2 "FFT field calculation with phasemap and PSD and BRD".

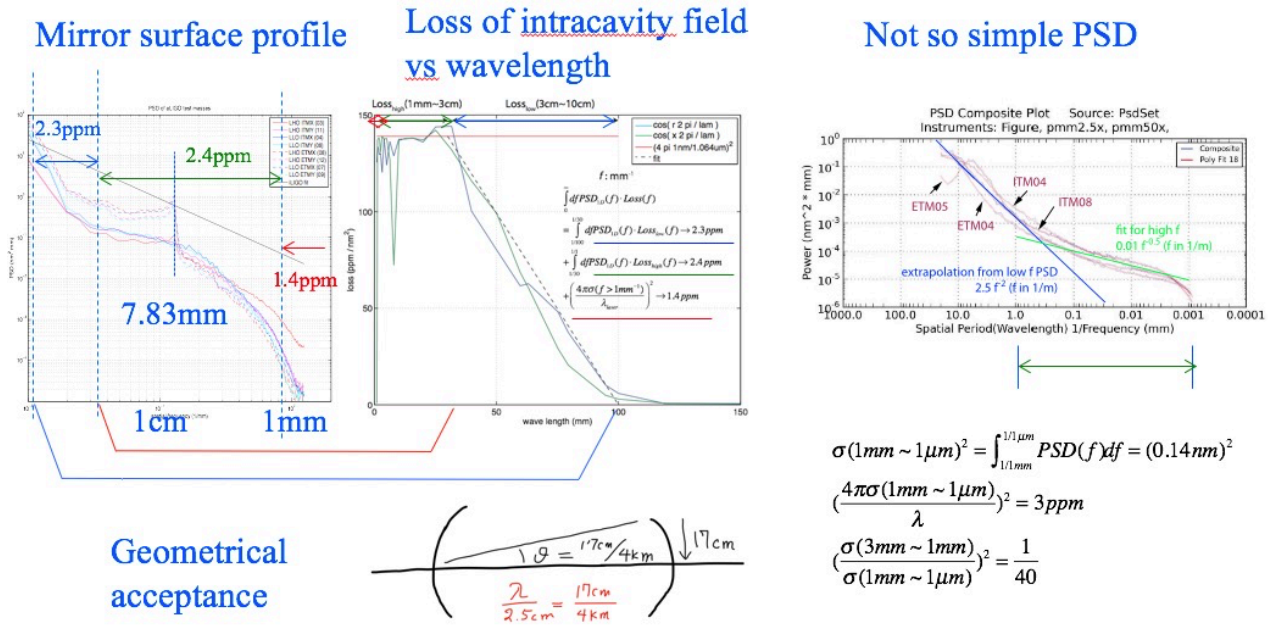

$$\sigma(1mm \sim 1\mu m)^2 = \int_{1/1mm}^{1/1\mu m} PSD(f)df = (0.14nm)^2$$

$$(\frac{4\pi\sigma(1mm \sim 1\mu m)}{\lambda})^2 = 3ppm$$

$$(\frac{\sigma(3mm \sim 1mm)}{\sigma(1mm \sim 1\mu m)})^2 = \frac{1}{40}$$

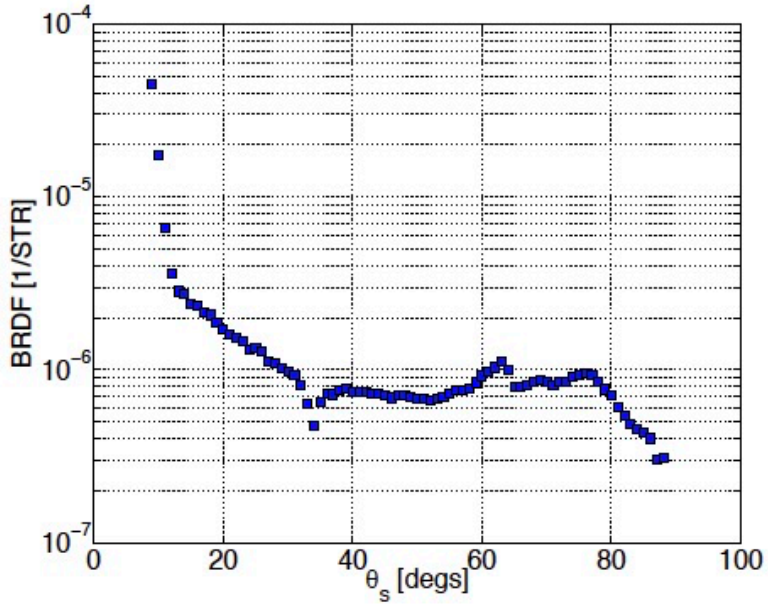

Fig. 9. BRDF versus scattering angle for the highly-reflecting mirror.

https://doi.org/10.1364/JOSAA.29.001722, LIGO-P1200030

2.5 Optical Level PD

BRDF measured by OpLev (ppm)

	L1	H1
ITMX	250	260

ITMY	500	420
ETMX	30	37
ETMY	43	28

3 Formulation

3.1 Fundamental expression

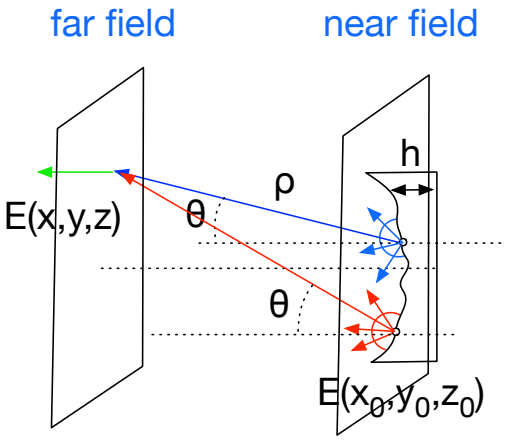

Huygen's integral

$$E(x,y,z)=\frac{i}{\lambda}\iint dx_0\,dy_0 E(x_0,y_0,z_0)\frac{\exp(-ik\rho)}{\rho}\cos(\theta)=E_0(x,y,z)+dF(x,y,z)$$

$$E(x_0,y_0,z_0)=(1+A(x_0,y_0,z_0))E_0(x_0,y_0,z_0)=E_0(x_0,y_0,z_0)+dF_0(x,y,z)$$

$$\Delta x=x-x_0,\ \Delta y=y-y_0,\ L=z-z_0,\ k=2\pi/\lambda$$

$$\rho=\sqrt{\Delta x^2+\Delta y^2+L^2},\ \cos(\theta)=L/\rho$$

$$dF_0(x_0,y_0,z_0)=A(x_0,y_0,z_0)E_0(x_0,y_0,z_0)$$

Fresnel approximation ($\theta^2 << 4/F$, F(Fresnel number) = $w_0^2/\lambda L$)

$$dF(x,y,z)=\frac{i}{\lambda}\iint dx_0\,dy_0 dF_0(x_0,y_0,z_0)\frac{\exp(-ik\rho)}{\rho}\cos(\theta)$$

$$\approx\frac{i}{\lambda L}\iint dx_0\,dy_0 dF_0(x_0,y_0,z_0)\exp(-ik\frac{\Delta x^2+\Delta y^2}{2L})$$

Fraunhofer approximation (Fresnel number << 1)

$$dF(x,y,z) \approx \frac{i}{\lambda L}\exp(-ik\frac{x^2+y^2}{2L})\iint dx_0\, dy_0 dF_0(x_0,y_0,z_0)\exp(ik\frac{x\cdot x_0 + y\cdot y_0}{L})$$

The Huygen's integral, calculating the far field by adding the near fields scattered on the source surface using the spherical wave propagation, is valid for wide varieties of aberration.

For a reflection by surface aberration, A = exp(2ikh) – 1, which can be approximated by 2ikh when the aberration h << wavelength λ, while it can be as large as -2 when h= λ/4. When a small area

G1501419-2, G1500262-6

3.2 Total scattered power and RMS and the GOLDEN RULE

3.2.1 formula

This formula applies for all aberrations. Golden rule is a formula calculating the total scattering by a mirror. Sec.3.6 discusses the relationship between the golden rule and the cavity loss.

$$\begin{aligned}
dP &= \iint dx\,dy\,|\,dF(x,y,z)\,|^2 \\
&= \frac{1}{(L\lambda)^2}\iint dx\,dy\iint dx_1\,dy_1\iint dx_2\,dy_2 dF(x_1,y_1)dF(x_2,y_2)^*\times \\
&\exp(i2\pi\frac{x(x_1-x_2)+y(y_1-y_2)}{L\lambda}) \\
&= \frac{1}{(L\lambda)^2}\iint dx_1\,dy_1\iint dx_2\,dy_2 dF(x_1,y_1)dF(x_2,y_2)^*(L\lambda)^2\delta(x_1-x_2)\delta(y_1-y_2) \\
&= \iint dx_0\,dy_0\,|\,E_0(x_0,y_0)\,|^2\,|\,A(x_0,y_0)\,|^2 \\
&= |\,E_0\,|^2\,\Delta S\frac{\iint dx_0\,dy_0\,|\,A(x_0,y_0)\,|^2}{\Delta S}
\end{aligned}$$

The last expression is the case when the aberration is in a small area, size of ΔS, where the unperturbed field amplitude E_0 is constant.

For a reflection with small aberration, $A \approx 2kh(x_0,y_0)$. And with the definition of

$$\sigma^2 = \frac{\iint dx_0\,dy_0\,|\,h(x_0,y_0)\,|^2}{\Delta S}$$

the relative scattering power, scattered power fraction with respect to the power hitting the area of the aberration becomes as follows.

$$\frac{dP}{|\,E_0\,|^2\cdot\Delta S} = (\frac{4\pi\sigma}{\lambda_{laser}})^2 = (\frac{4\pi 10^{-9}}{\lambda_{laser}})^2\sigma[nm]^2 = 140\,ppm\cdot(\frac{\sigma[nm]}{\lambda_{laser}/\lambda_{1.064}})^2$$

This is called the GOLDEN RULE.

This σ is the rms in the measured area. The rms monotonically becomes larger when the measured area becomes wider. This can contribute part of the observation that the cavity loss becomes smaller when a cavity is designed with smaller beam size.

T1000154

3.2.2 Total scattering is proportional to number of defects, not N^2

It is a simple fact that the total power of the far field is the same as the total power of the near field. The formula above shows this by expressing the total scattered power, dP, by the mirror surface quantity. From this, it can be concluded that the scattered field power by a surface with multiple small size defects is proportional to the number of defects, not the square of defects. As is discussed below, the distribution of the far field power can be affected by the interference of fields scattered by multiple defects, especially populated nearby each other, the total power is not affected by the interference.

3.2.3 Total scattering is proportional to the power interacting with the defect

Another important fact is that the scattered power is limited by the power which interacts with the aberration, $|E_0|^2 \Delta S$. For a Gaussian field with width of w interacting with a circular defect with radius of a, $|E_0|^2 \Delta S = 2(a/w)^2$. In order to cause 1ppm scattering for a Gaussian field with 5cm radius by a single defect, the defect size radius should be at least ~50μm.

3.3 Difference between continuous aberration and point defect

Wide spread periodic defects reflects the field into one direction by the interference of reflections in a wide area. See 3.5 below.

Reflection by a small size defect distributes uniformly in $\theta \ll \lambda_{laser} / a$, and drops down outside due to negative interference.

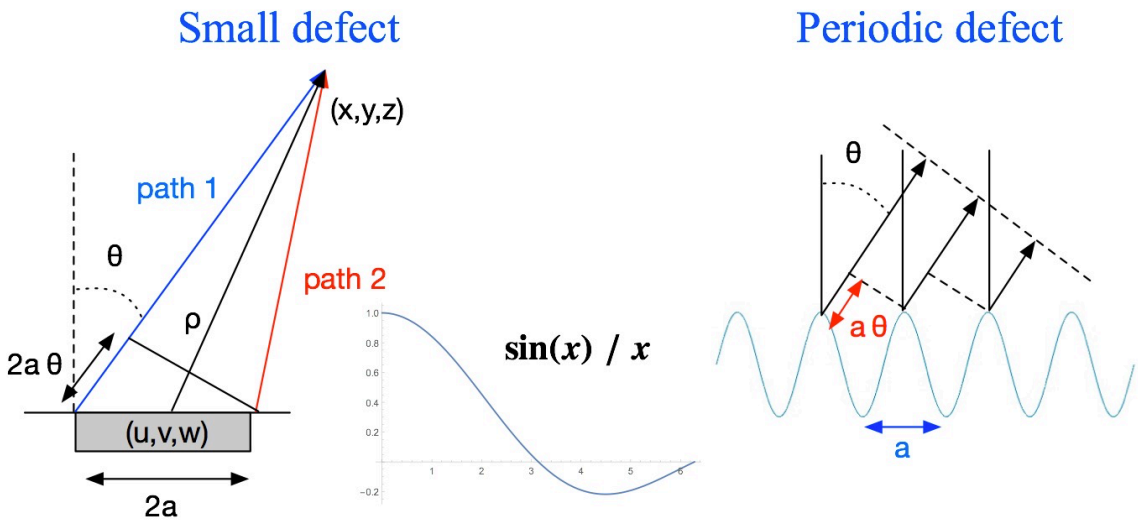

$$\mathrm{Exp}[-i\,k\,\rho] = \mathrm{Exp}[\,i\,k\,(x\,u + y\,v)\,/\,L\,] = \mathrm{Exp}[i\,k\,(\theta_x\,u + \theta_y\,v)];$$

$$\int_{-a}^{a} \mathrm{Exp}[i\,k\,\theta_x\,u]\,du = 2\,a\,\frac{\mathrm{Sin}[\,k\,\theta_x\,a]}{k\,\theta_x\,a}$$

$$a\,\theta = \lambda$$

G1501419-6

3.4 Scattering power distribution by continuous aberrations

This applies to aberrations which can be characterized by amplitude or power spectral density, i.e., aberrations which distributions in a wide area on the reflecting surface.

$$dF(x,y,z) = \sqrt{\frac{2}{\pi}}\,\frac{(-2k)}{\lambda L\, w(z1)}\, e^{-\frac{ik\left(x^2+y^2\right)}{2L}-ikL} \int_{-\infty}^{\infty}\int_{-\infty}^{\infty} \Delta(f_u,f_v)\,\delta\left(f_u-\frac{\theta_x}{\lambda},a\right)\delta\left(f_v-\frac{\theta_y}{\lambda},a\right) df_u\, df_v;$$

ASD: $$h[u,v] = \int_{-\infty}^{\infty}\int_{-\infty}^{\infty} \Delta[f_u,f_v]\, e^{-i2\pi(u f_u+v f_v)}\, df_u\, df_v;\ \mathrm{Exp}[i2kh] \simeq 1+i2kh;\ A = i2kh;$$

$\lambda_S \rightarrow \theta_{\text{far field}}$: $$\theta_x = \frac{x}{L};\ a = \sqrt{i\,\frac{1}{\pi\lambda L}\,\frac{w2}{w1}\exp(-(\eta(z2)-\eta(z1)))};\ \delta\left(f_u-\frac{\theta}{\lambda},a\right) = \frac{\exp\left(-\frac{\left(f_u-\frac{\theta}{\lambda}\right)^2}{a^2}\right)}{\sqrt{\pi}\,a};\ \int_{-\infty}^{\infty}\delta(f,a)\,df = 1;$$

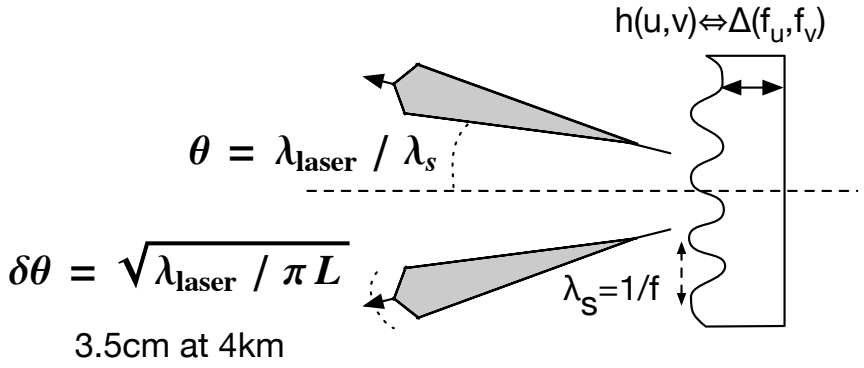

G1501419-3

The following plot shows the power flow calculated using FFT to compare numerical calculations and the above analytic approximation. For all cases, a perfect Gaussian field with width of 6.2cm is reflected by a mirror with RoC of 2245m. The mirror surface has an aberration of $\sqrt{2}\cos(2\pi r/\lambda s)$ (nm) is placed on it.

Red lines are power distributions after 4km propagation using λs = 1cm, while blue lines using λs = 5mm at 4km and 2km. Red solid and dashed lines are to show the finite aperture size effect, and blue lines to show the dependence on the propagation distance. At each distribution, three vertical lines corresponding to L x ($\theta \pm \delta\theta$) are shown.

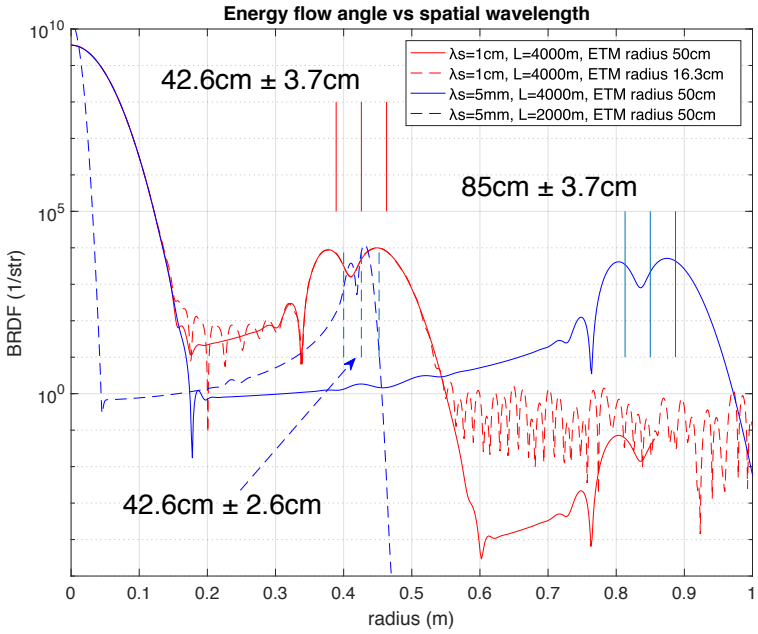

3.5 Spatial wavelength of aberration and cavity loss

3.5.1 Outline

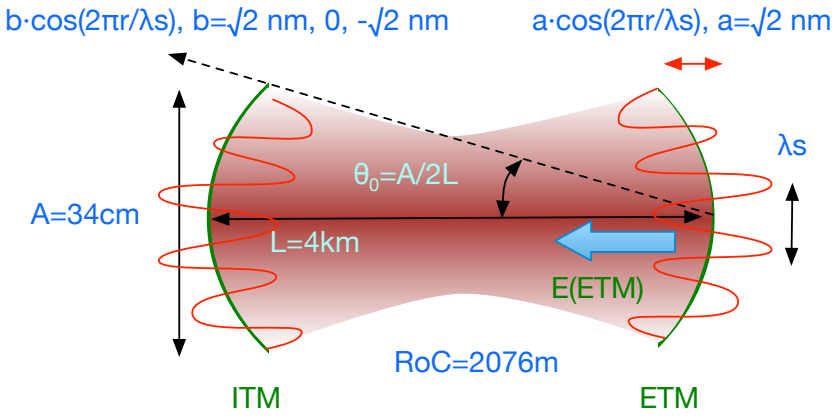

The following plot is the round trip loss, calculated by Hankel simulation (T1000254), in a FP cavity with aberration with height 'a cos(2 π r /λ_s)' on ETM and 'b cos(2 π r /λs)' on ITM. a is chosen to be √2 nm to make the rms = 1nm. b(ITM) is chosen to be √2 nm, 0nm and -√2 nm. The horizontal axis of the plot is the spatial wavelength λ_s of the aberration on ETM and ITM. The cavity is locked at each spatial aberration. When b is not 0, the loss is divided by 2 to make the loss per mirror.

As is shown in Sec.3.5, the field scatted by an aberration on ETM with spatial wavelength shorter than the cutoff wavelength $\lambda_0 = \lambda_{laser} / \theta_0 = 2\ L\ \lambda_{laser} / A$ is scattered outside of ITM. This cutoff wavelength is 5cm for A=34cm. This is a simplified argument. The real scattering is more complex and there is no sharp transition at any wavelength.

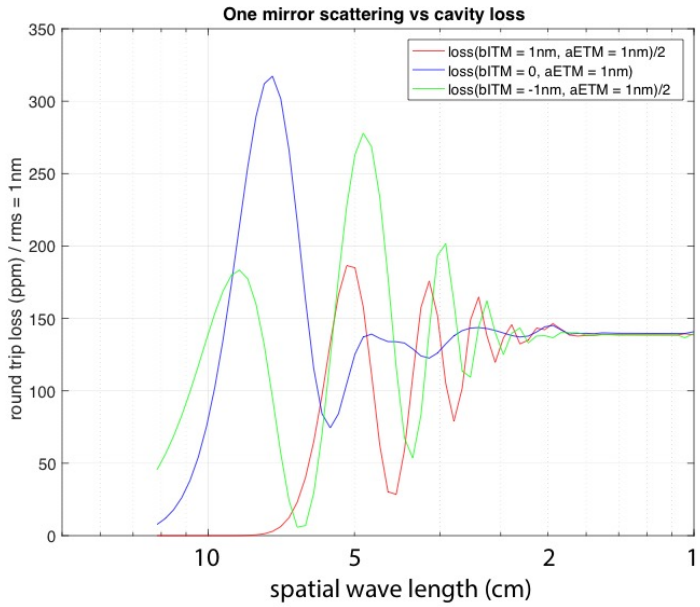

3.5.2 Short wavelength region :

At $\lambda s \ll \lambda_0$, all reflected field by the aberration on ETM goes out of ITM, so the loss is 140ppm for λ_{laser} =1.064μ, as is predicted in Sec 3.3. The solid angle of the ITM seen from ETM is $\Delta S(A)= \pi (A/2L)^2$ =6e-9, and the fraction of the scattered field hitting the ITM is negligible.

As is shown in the plot, the loss in three different cavity configurations (different b(ITM) values) are the same in this short wavelength region (λs ~ 1cm).

3.5.3 Medium wavelength region :

In the region λs ~ λ0, the value of the round trip loss varies. This is because part of the field reflected by the aberration with this wavelength region hits ITM and that will contribute to form the intra cavity field. The stationary cavity field depends on the cavity configurations, and the loss estimation using the simple golden rule does not work.

The following plot is the higher order mode fraction of the field on ETM going toward ITM. In the short wavelength region, the HOM fraction is the same as the fraction of the loss. But, in the medium wavelength region, the HOM fraction depends on the aberration on ITM, which in turn affects the round trip loss. The HOM fraction is the smallest when both TMs have the same aberration, i.e, a(ETM) = b(ITM) = √2 nm, and the fraction is the largest when a(ETM) = -b(ITM). The detail of this mechanism is discussed in T0900306.

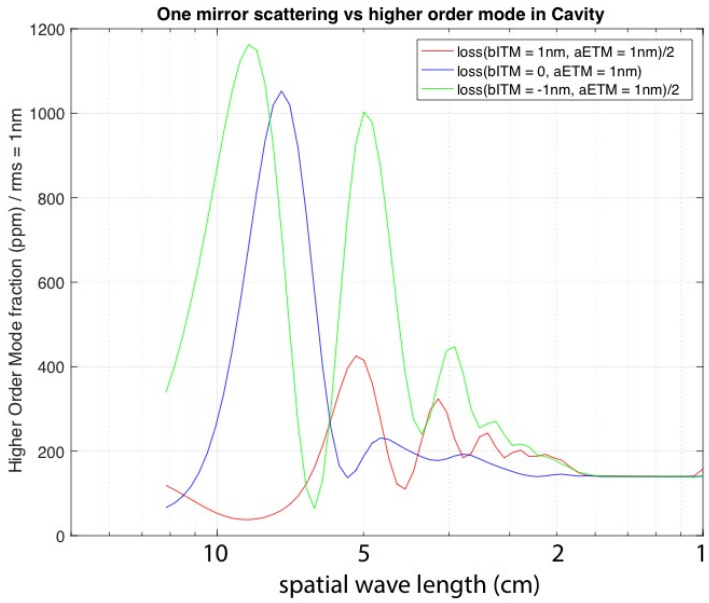

3.5.4 Long wavelength region :

In the long wavelength region, $\lambda s \gg \lambda 0$, the scattered fields are all captured in the cavity and the aberration affects the higher order mode excitation or deformation of the parameters of the base resonating mode, like the change of RoC of the Gaussian field.

This is independent on the aberration for a given cavity.

3.6 Scattering power distribution by isolated aberrations or point defects

For a reflector with a simple shape, circular disk and rectangular shape, Formula in 3.2 can be explicitly calculated.

The analytic formulas of the scattered fields and power distributions for these two cases are shown below. The power distribution has a flat plateau at the center and then periodic and dumping structure outside.

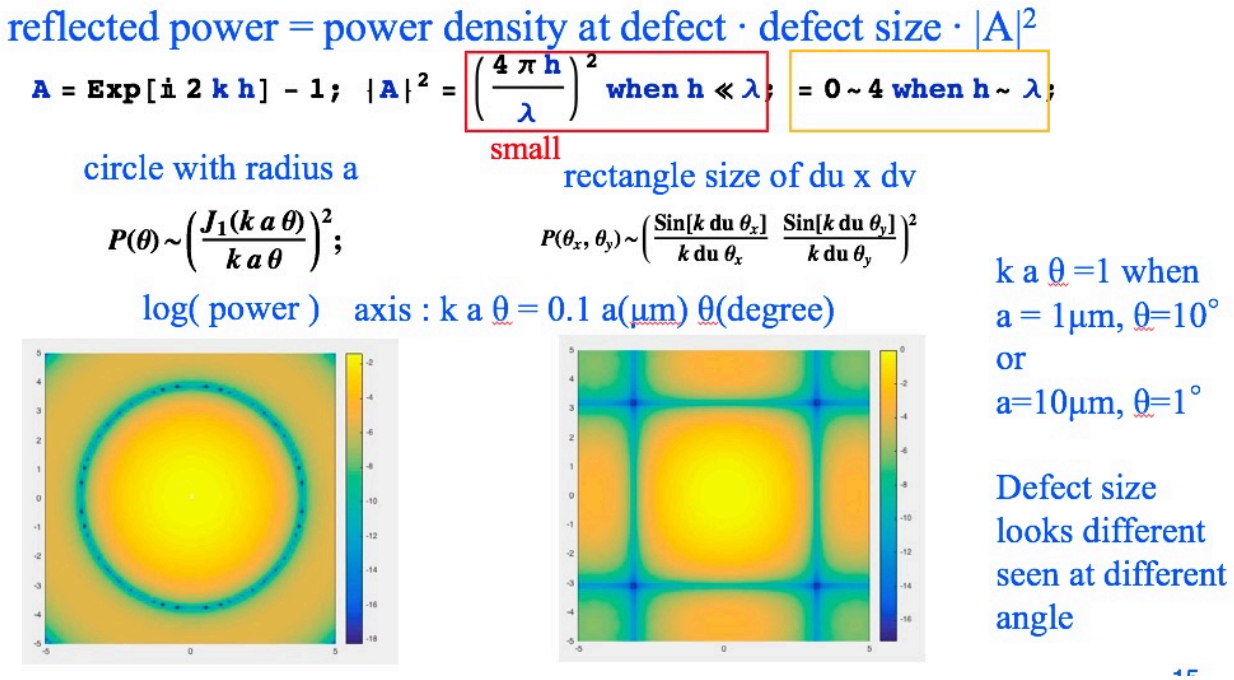

G1601678-15

Depending on the shape and size of the defect, the power distributions are different. The following plot compares the angular distribution of the power reflected by circular disks with different radiuses, together with the Rayleigh scattering.

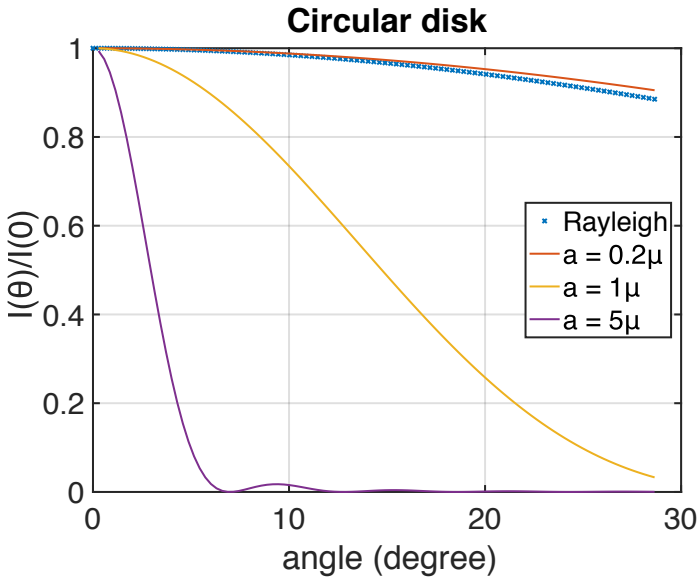

The following plot shows the energy fraction which goes out of an cone with a given opening angle – a. la. integrating sphere – for three different kinds of reflectors.

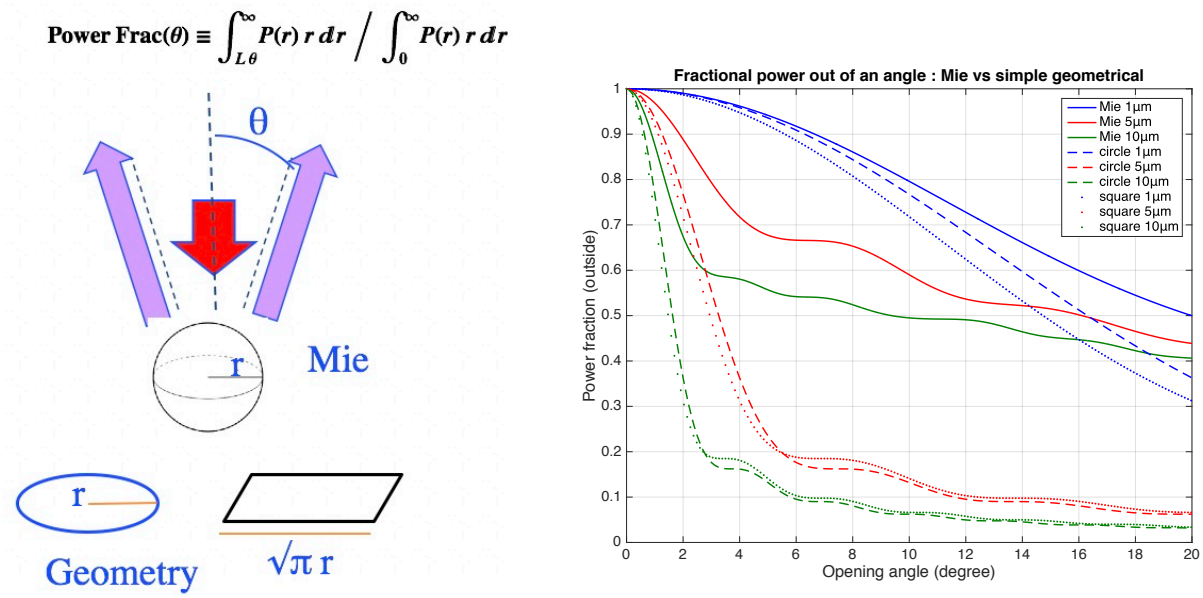

G1601678-7

At far distance from the scattering surface, one continuous defect, like a solid square, and group of small defects clustered in an area cannot be distinguished. The following distributions compares far field power distributions by a solid square reflector (top-left) and by a cluster of small reflectors of circular shapes randomly distributed in the same area as the solid square (bottom-left). The power distribution by a cluster of small defects is not as clean rectangular as by a solid reflector, but very similar.

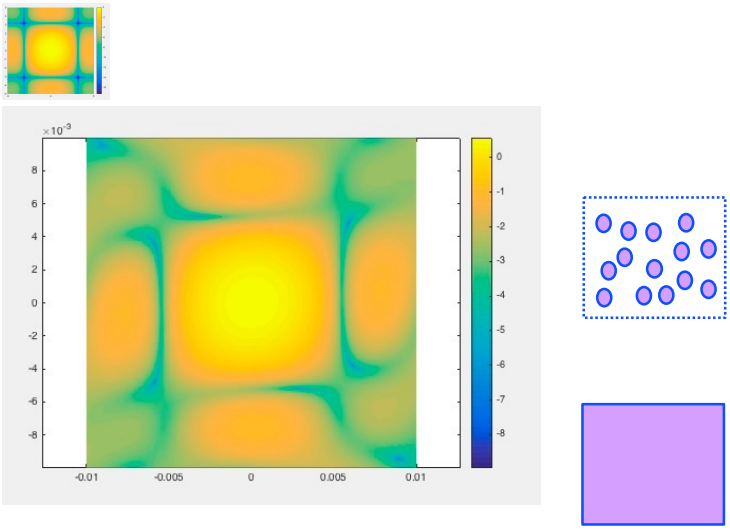

G1501419-9

4 Miscellany

4.1 Diffraction, Finite size mirror effect, Airy Ring

Even when the mirror surface is perfect, the finiteness of the mirror size induces field distortion, known as Airy ring. The following plot shows the BRDF of the field, or dP/dxdy / ($1/L^2$) / Ptotal

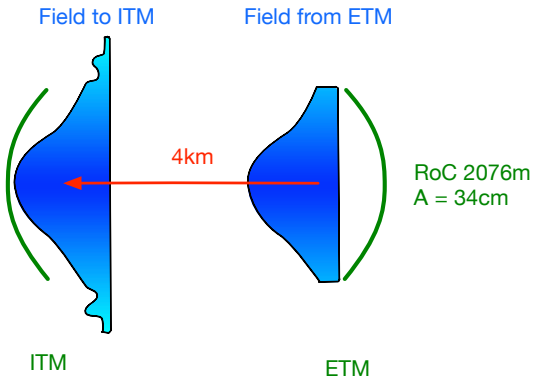

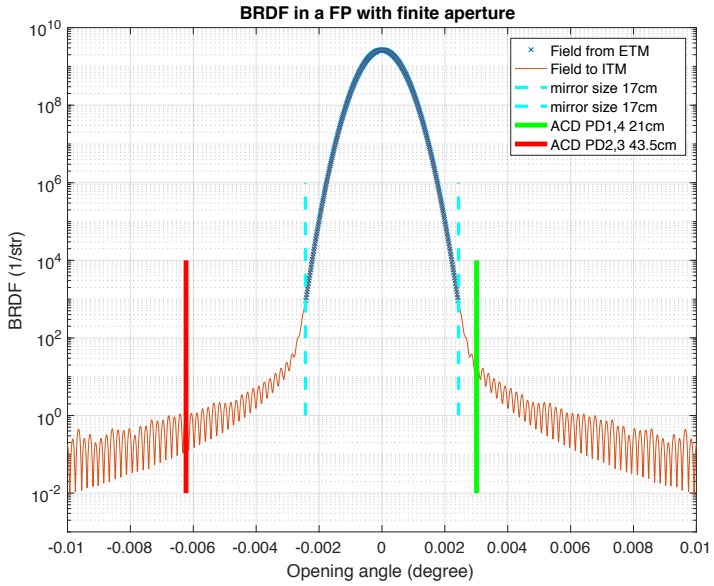

The orange line is the field on ITM when a Gaussian field propagates from ETM with finite aperture A of 34cm, shown by a blue cross line. The oscillation of the orange line out of 20cm is the Airy ring.

The field propagating to a mirror out of the aperture, outside of two vertical cyan dashed lines, is lost. For the aLIGO arm cavity, the round trip loss is 0.6ppm when the aperture size of 34cm is used, while it is 1.9ppm when the actual coated size of 32.6cm is used.

The field on ITM with the Airy ring can be calculated explicitly using the Fraunhofer approximation for a plane wave and the angular dependence of the BRDF is

$$BRDF(\theta) \propto \frac{1}{\theta^3}(1 - \sin(k\,A\,\theta))$$

The period of the oscillation is k A θ = 2 π, or, θ = λ / L = 1.7e^{-4} degree. This approximation using the plane wave is a good approximation of the numerical result shown in the plot for the Gaussian propagation.

The green and red vertical line show the locations of the ACD PDs at 21cm and 43.5cm. As can be seen from this plot, the effect of the mirror size affects the power distribution and the power is much larger than the simple Gaussian tail. Because of this, these PDs cannot be used to study the aberration of the mirror surface.

The loss due to the finite size of the test masses is small, less than 1ppm, for the main TEM00 mode, and the non Gaussian tail is visible only just around the test mass.

When one of the mirror surface changes a little bit by thermal effects, this ring radius can change a little bit. But, the observed power by a PD at a fixed radius may change a lot due to this rapid oscillation. The following is the change of power density when the input power changes from 1W to 40W.

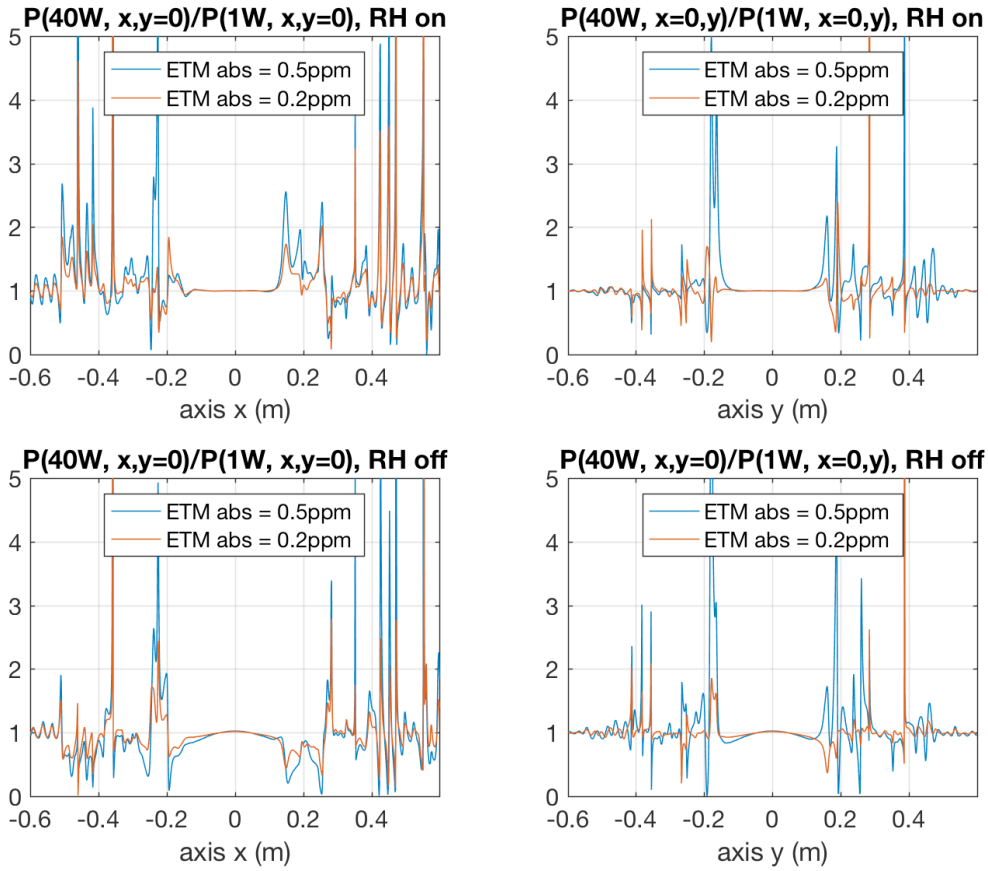

The following is the data of iLIGO, measured by Valera, and clear oscillation is observed.

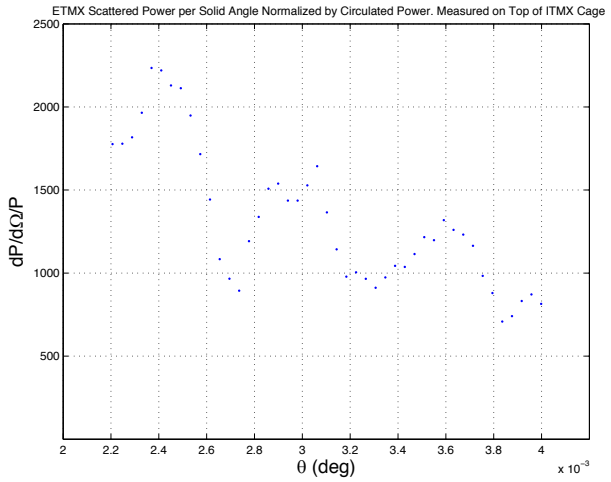

4.2 FFT field calculation with phasemap and PSD and BRDF

The BRDF and PSD are related as (formula in Sec 3.4, T070082, or "Optics Scattering" by Stover)

$$BRDF(\theta) = (\frac{4\pi}{\lambda^2})^2 PSD_{2d}(f) = (\frac{4\pi}{\lambda^2})^2 D \cdot PSD(f)_{1d} / f$$

$$PSD_{1d}(f) \sim f^{-C}$$

$$D = \Gamma(\frac{C+1}{2}) / 2\sqrt{\pi}\Gamma(\frac{C}{2})$$

D=1/4 for C=2, D=1/2π for C=1

The following plot shows typical polished surface PSDs of aLIGO test masses.

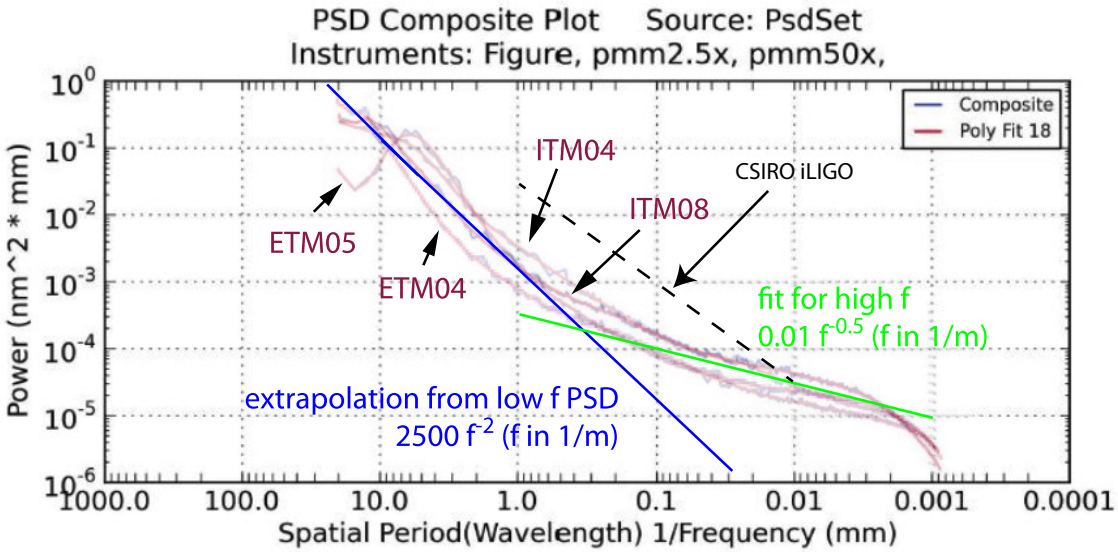

Using the fitting in the region around 1mm~1cm, PSD(f(m)) = $2500e^{-21}$ f^{-2}, corresponding BRDF is calculated as

$$BRDF(\theta) = (\frac{4\pi}{\lambda_{laser}^{\ 2}})^2 \frac{1}{4} \cdot 2500e^{-21} f^{-3}$$

$$= (\frac{4\pi}{\lambda_{laser}^{\ 2}})^2 \frac{1}{4} \cdot 2500e^{-21} \lambda_s^3 \quad ; \text{f}=1/\lambda_s \text{, } \theta=\text{r/L}=\lambda_{laser} / \lambda_s$$

$$= (\frac{4\pi}{\lambda_{laser}^{\ 2}})^2 \frac{1}{4} \cdot 2500e^{-21} \lambda_{laser}^3 \theta^{-3} = 9e^{-11} \cdot \theta(rad)^{-3}$$

$$= (\frac{4\pi}{\lambda_{laser}^{\ 2}})^2 \frac{1}{4} \cdot 2500e^{-21} (\frac{\lambda_{laser} L}{r})^3 = 6 \cdot r(m)^{-3}$$

(ref. R.Weiss T000011 BRDF(iLIGO ITM by CSIRO) = $8e^{-8}$ / θ^{-2})

The spatial wavelength is replaced by the corresponding field position, r, on the mirror at L=4km away.

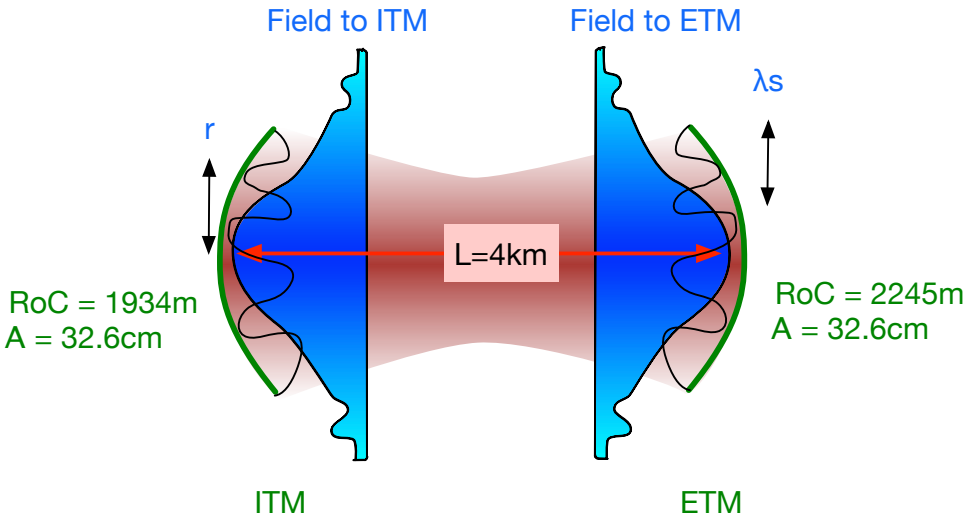

The following plot shows BRDF of the field going to ITM and to ETM in a resonating cavity. It shows log of BRDF vs r^2, and a straight line around r=0 means the Gaussian power distribution. The BRDFs marked as "with map" are the average of fields in the 4 arms in H1 and L1.

The fields are calculated using a FFT simulation with spatial resolution of 1mm, which will give reasonable result for λ_s >~ 4 mm. The phasemap can possibly have inefficiency in the region for λ_s < 2mm.

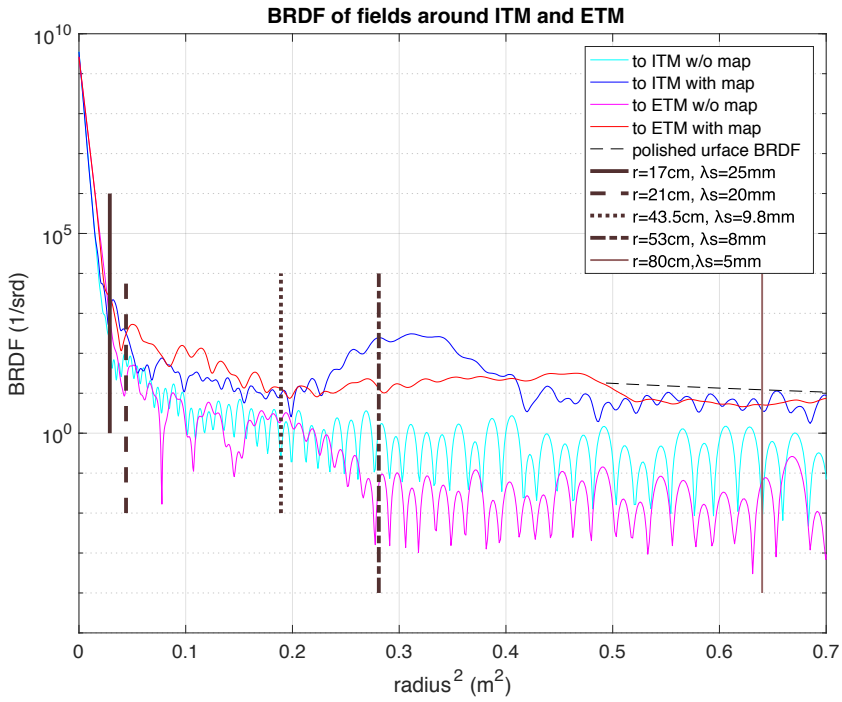

The round trip loss in 4 arms at H1 and L1 are shown, using the aperture size of 32.6cm. When the mirror maps are not used, the loss is 1.9ppm. These numbers are almost the same when the FFT grid size of 2mm is used, instead of 1mm.

	X arm	Y arm
H1	20ppm	16ppm
L1	18ppm	15ppm

The BRDF based on the polished surface PSD is also shown in the same plot by a black dashed line. PSD and BRDF do not have full information, non-axisymmetric components and variation of RMS from location to location, etc, and the prediction is, sort of, back of the envelope calculation. The coated surface PSD is larger than the PSD of uncoated surface. So the comparison in the plot is not quite quantitative result, but still, it shows that two calculations are consistent order of magnitude.

The angular dependence of the BRDF in a cavity with phasemaps in the region $r^2 = 0.5 \sim 1\ m^2$, or $r = 0.7 \sim 1m$, or $\lambda_s = 6 \sim 4mm$, or $\theta = 0.01 \sim 0.014°$, is around θ^{-3}, which happens to be the same as the tail by the finite aperture effect.

Important and to be used in $\lambda_s > 5mm$, or $r < 0.8m$ or $\theta < 0.01°$.

4.3 OpLev PD

This is a simple estimation of the BRDF, in the region of interest. I got dimension from D0901464-v6 aLIGO Systems Layout LLO Y-End Station_Lo …pdf.

In this region, the scattering estimation using phasemap does not work, because 1mm spacing corresponds to 0.06 degree.

The scattering in this region will come from continuous roughness and point scattering. Both of these are not well known.

One rough estimation of the continuos roughness is to assume that the PSD of the coated surface is proportional to that of the polished surface. The TIS data shows that the measured loss is 3-5 times of the loss based on polished surface RMS in the wavelength region corresponding to the TIS spacial coverage.

A rough fit of the PSD of polished surfaces of ITM and ETM is PSD(f) = 10^-22 f^-2/3 (f in 1/m and PSD in m^3).

BRDF from continuous roughness is 1/2pi (4pi/lambda)^2 PSD(theta/lambda) / lambda =8 pi / lambda^3 PSD.

The following plot shows he scattering by this continuous roughness x 3 and the scattering from point roughness 30ppm / 2pi.

The polished surface RMS with lambda = 100micron ~ 1micron of ITM is higher than that of ETM by factor 2, so the loss could be higher by factor 4.

When compared with the OpLev power (alog 28668) data, this estimation is factor of several lower for both ITM and ETM.

The upper limit of the scattering into the Pcal periscope can be estimated by the OptLevel BRDF, if OptLevel data error is reasonably small.

I will think more carefully.

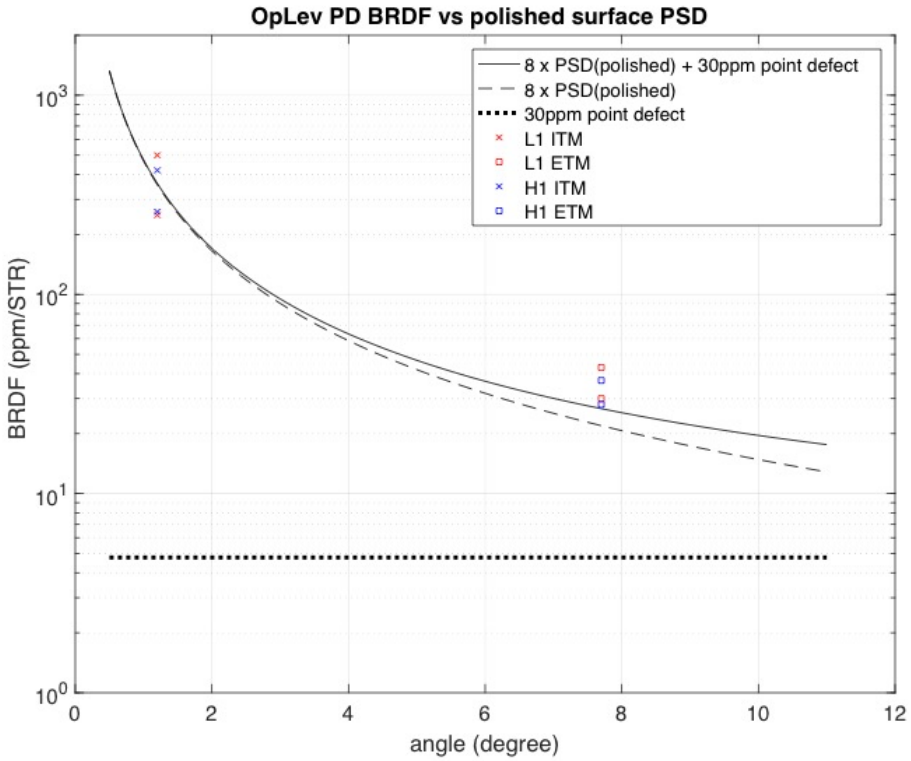
OpLev PD BRDF vs polished surface PSD
8 x PSD(polished) + 30ppm point defect
8 x PSD(polished)
30ppm point defect
L1 ITM
L1 ETM
H1 ITM
H1 ETM
BRDF (ppm/STR)
angle (degree)

5 FUROKU

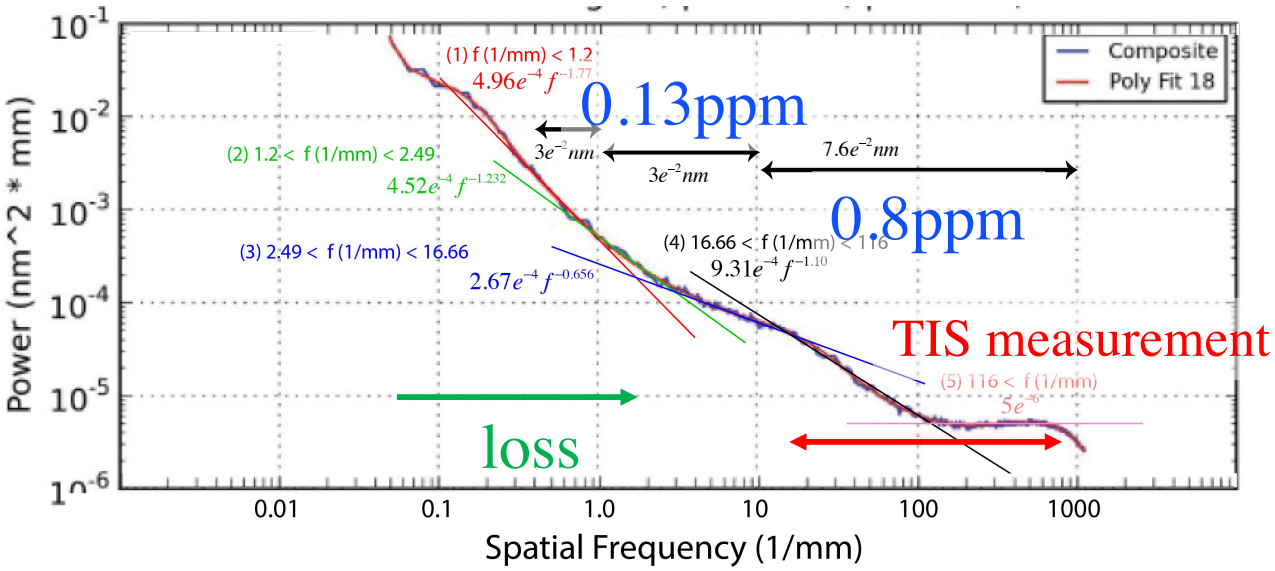
Composite
Poly Fit 18
(1) f (1/mm) < 1.2
$4.96e^{-4} f^{-1.77}$
0.13ppm
$3e^{-2}nm$
$3e^{-2}nm$
$7.6e^{-2}nm$
(2) 1.2 < f (1/mm) < 2.49
$4.52e^{-4} f^{-1.232}$
0.8ppm
(3) 2.49 < f (1/mm) < 16.66
$2.67e^{-4} f^{-0.656}$
(4) 16.66 < f (1/mm) < 116
$9.31e^{-4} f^{-1.10}$
TIS measurement
(5) 116 < f (1/mm)
$5e^{-6}$
loss
Power (nm^2 * mm)
Spatial Frequency (1/mm)

$$E_{ref} = E_{ref}^0 \exp(i\omega t - ikz)\cdot\exp(2ikf(x,y))$$
$$= E_{ref}^0 \exp(i\omega t - ikz)(1-2(kf)^2) + E_{ref}^0 \exp(i\omega t - ikz)i2kf$$

dF

$$f(x,y) = \sum_{nx,ny} a_{nx,ny}\sin(n_x\omega_x x + n_y\omega_y y + \varphi_{nx,ny})$$

$$dF = E_{ref}^0 k \sum_{nx,ny} a_{nx,ny}(\exp(i\Phi_{nxny}^+) - \exp(i\Phi_{nxny}^-))$$

$$\sigma^2 = \frac{\iint dx\,dy f^2}{S}$$

Small size aberration

$$dW = \iint dx\,dy \left|E_{ref}^0\right|^2 4k^2 f^2$$

$$= P_{ref}^0 \left(\frac{4\pi\sigma}{\lambda}\right)^2 S$$

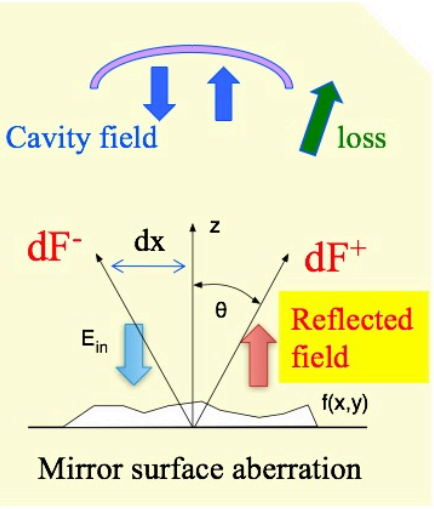

* Periodical aberration scatters to a fixed angle

$$\theta \sim n\sqrt{\omega_x^2 + \omega_y^2}\,/\,k \sim n\cdot\lambda/a,\quad dx = L_{cav}\cdot\theta \sim L_{cav}\cdot\lambda/a$$

* Small size aberration scatters back spherically

$$loss = (1-(\text{mirror size} / \text{cavity length})^2)\bullet dW$$

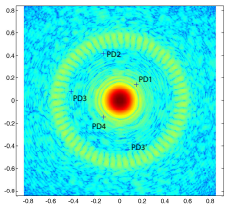

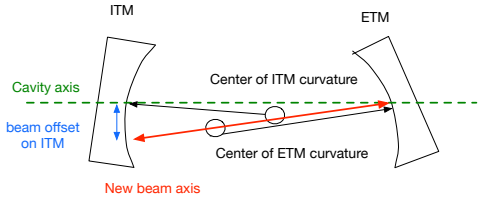

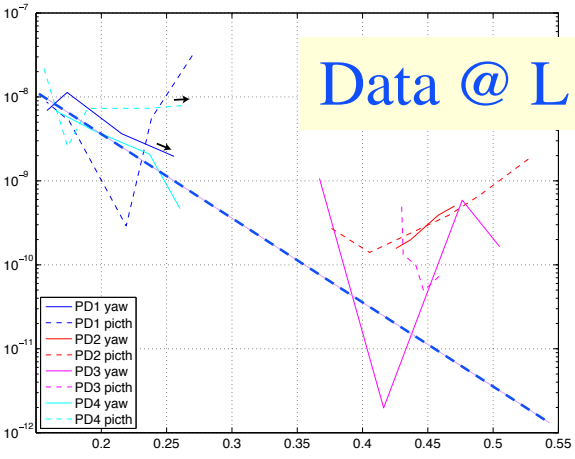

Data @ L1

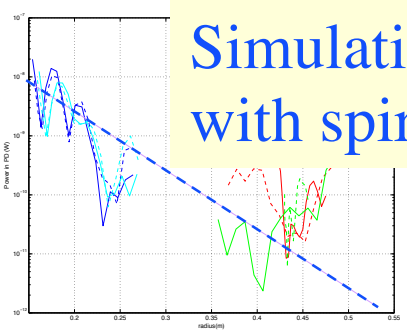

Simulation with spiral

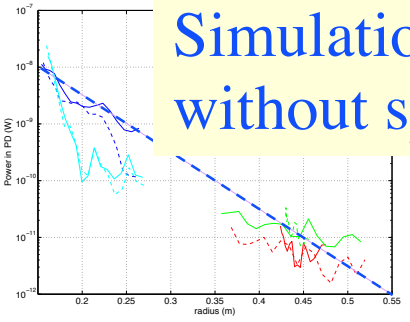

Simulation without spiral

Distance of PD from center